JUN Oncogene Amplification and Overexpression Block Adipocytic Differentiation in Highly Aggressive Sarcomas

Odette Mariani,[1,2] Caroline Brennetot,[1,2] Jean-Michel Coindre,[3] Nadège Gruel,[4] Carine Ganem,[1,2] Olivier Delattre,[1,2] Marc-Henri Stern,[1,2] and Alain Aurias[1,2,*]

[1] Institut Curie, Genetics and Biology of Cancers, 26 rue d'Ulm, 75248 Paris cedex 05, France
[2] INSERM U830, F-75005 Paris, France
[3] Institut Bergonié, Department of Pathology, 229 cours de l'Argonne, 33076 Bordeaux cedex, France
[4] Institut Curie, Department of Transfert, 26 rue d'Ulm, 75248 Paris cedex 05, France
*Correspondence: alain.aurias@curie.fr
DOI 10.1016/j.ccr.2007.02.007

SUMMARY

The human oncogene *JUN* encodes a component of the AP-1 complex and is consequently involved in a wide range of pivotal cellular processes, including cell proliferation, transformation, and apoptosis. Nevertheless, despite extensive analyses of its functions, it has never been directly involved in a human cancer. We demonstrate here that it is highly amplified and overexpressed in undifferentiated and aggressive human sarcomas, which are blocked at an early step of adipocyte differentiation. We confirm by cellular and xenograft mouse models recapitulating these sarcoma genetics that the failure to differentiate is dependent upon *JUN* amplification/overexpression.

INTRODUCTION

Undifferentiated soft-tissue sarcomas are the most frequent malignant mesenchymal tumors in adults. Patients with these tumors have a poor prognosis, with a 5 year survival rate of around 60%. We have previously shown that a subgroup of these tumors exhibited constant high-level amplification of the 12q14 chromosome region encompassing the *MDM2* locus and the *CDK4* locus (Chibon et al., 2002; Coindre et al., 2003)—genetic characteristics strongly reminiscent of those observed in well-differentiated liposarcoma (WDLPS), an adipocytic tumor with good prognosis (Forus et al., 1993; Khatib et al., 1993). In undifferentiated sarcomas, however, the 12q amplification is always associated with amplification of either 6q23 or 1p32, a feature never observed in WDLPS, except in their undifferentiated relapses. This suggests that these undifferentiated tumors might correspond to undifferentiated liposarcomas, and that lack of differentiation could be related to secondary amplification of certain target genes in the 1p32 or 6q23 chromosome bands (Chibon et al., 2002; Coindre et al., 2003; Heidenblad et al., 2006).

We recently demonstrated that 6q23 amplifications likely target *MAP3K5*, a gene encoding a protein in the JNK signaling pathway (Chibon et al., 2004). Here, we demonstrate that the target of 1p32 amplifications is the *JUN* oncogene, and that overexpression of this gene closely correlates with the undifferentiated state of the tumors. This oncogene, cellular homolog of the v-Jun avian sarcoma virus 17, was isolated in 1987 (Bohmann et al., 1987) and more precisely characterized in 1988 (Angel et al., 1988; Hattori et al., 1988). It encodes a component of the AP-1 complex and is consequently involved in a wide range of pivotal cellular processes, including cell proliferation, transformation, and apoptosis (Shaulian and Karin, 2002). Nevertheless, despite extensive analyses of its functions, it had previously never been directly involved in a human cancer.

SIGNIFICANCE

We have demonstrated that amplification and overexpression of the oncogene *JUN* in human liposarcomas lead to an undifferentiated and aggressive tumor phenotype. Besides the opportunity to better understand the biology of the undifferentiated sarcomas and the connections between proliferation and differentiation in mesenchymal tumors, these findings provide also a starting point for the development of new diagnostic tests for and clinical management of these aggressive human sarcomas. They provide the foundation for targeted gene therapy designed to control these tumors. The xenograft model described here appears as a particularly efficient tool for testing new gene-targeted drugs.

RESULTS AND DISCUSSION

JUN Is the Only Known Gene in the Minimal 1p32-Amplified Region

A preliminary analysis of allelic imbalances in 1p32 microsatellite loci was performed on tumor DNAs obtained from ten undifferentiated sarcomas (T1–T10) with amplified 1p32 and 12q14 regions. This allowed us to locate the amplified 1p32 region between microsatellite markers D1S200 and D1S499, with a putative minimal region between D1S2869 and D1S2737 (data not shown) corresponding to coordinates chr1:58372500–60938037 in the Human May 2004 Assembly at UCSC. To refine this location, we then designed a dedicated BAC-PAC array corresponding to this region. For this purpose, we selected 22 BAC-PAC clones in the putative minimal region and 15 clones in the two flanking regions, as well as 85 clones from 6q23 and 12q14 bands. This array was then used to analyze the ten tumors with 1p32 amplification by CGH. Eight loci, covering 736 kb on the 1p32 region (coordinates on chr1:58872559–59608936), were found amplified in all tumors (Figure 1A). A single known gene, *JUN*, as well as spliced ESTs and part of a coding sequence (FLJ10986), are located in this region, indicating that *JUN* could be the target of the amplicon. Genomic amplification of the *JUN* locus was confirmed by fluorescence in situ hybridization (FISH) on frozen tissue sections from three tumors, which all had a high copy number of *JUN* loci in all tumoral cells when compared to a control unamplified locus (Figure 1B).

JUN Is Overexpressed at the RNA and Protein Levels in Tumors with the 1p32 Amplicon

To investigate the consequences of this genomic amplification on the expression of *JUN*, the ten tumors with the 1p32 amplicon were studied by transcriptome analysis on Affymetrix U133 Plus 2.0 microarrays. They were compared to 13 tumors without 1p32 amplification on array CGH analysis (five WDLPS with 12q14 amplification, and eight undifferentiated sarcomas with 12q14 and 6q23 amplification). Relative overexpression of *JUN* was demonstrated by real-time PCR analysis, with a good correlation ($R^2 = 0.69$) between the expression levels and the genomic amplification levels previously observed in array CGH assays (Figure 2A). These data were confirmed by transcriptome analysis on Affymetrix Human Genome U133 Plus 2.0 chip. The expression levels of the other amplified coding sequence (FLJ10986), as well as those of DA310828 and BG215747 ESTs, were not strictly correlated with their genomic amplification status, suggesting that they are not the target genes (data not shown). Total protein extracts were analyzed by western blot of ten tumors with the 1p32 amplicon (T1–T10), three WDLPS (T11–T13), and one tumor with 6q23 amplicon (T15). JUN protein levels were vastly increased in tumors with *JUN* amplification/overexpression, and in tumors with 6q23 amplification (Figures 2B and 2C). Phosphorylation of JUN on serine 63 was increased in most tumors with 1p32 amplicon and in the tumor with 6q23 amplicon (T15). Protein levels

of JNK and phospho-JNK were similar in all undifferentiated and well-differentiated samples (data not shown).

We next screened the tumors by using immunohistochemistry to detect JUN protein overexpression on paraffin-embedded tissue sections. As shown in Figure 2D, all tumors with *JUN* overexpression stained strongly positive for JUN protein, with intense labeling of the nuclei. By contrast, JUN could not be detected in WDLPS, which have no 1p32 amplification. These data demonstrate that *JUN* amplification directly leads to its overexpression at both the RNA and protein levels, strongly suggesting that *JUN* is the target of 1p32 amplification in human sarcomas.

Genes Involved in Terminal Adipocytic Differentiation Are Not Activated in Tumors with *JUN* Overexpression

To test the hypothesis that *JUN* overexpression blocks adipogenesis, we analyzed by real-time PCR the expression levels of genes that are induced sequentially during adipogenesis: *SREBP1*, *C/EBPβ*, *C/EBPα*, *PPARγ2*, *LPL*, and *Adipsin* (Cowherd et al., 1999). The ten tumors with *JUN* overexpression were compared to three WDLPS with 12q14 amplification and three undifferentiated tumors with 12q14 and 6q23 amplification (T14–T16). As shown in Figure 3A, *SREBP1* and *C/EBPβ* were expressed in the three groups of tumors. By contrast, expressions of *C/EBPα* and *PPARγ2*, which are direct targets of *C/EBPβ*, and of *LPL* and *Adipsin* were absent from most undifferentiated tumors, and in particular from those with *JUN* overexpression, suggesting that the *C/EBPβ* transcriptional network is impaired in poorly differentiated liposarcomas. In agreement with our hypothesis, it is noteworthy that the T7 tumor, which exhibits the lowest *JUN* amplification/overexpression, has the highest expression levels of *SREBP1*, *C/EBPβ*, and *Adipsin* among the undifferentiated liposarcomas. Affymetrix U133 Plus 2.0 microarrays (Figure 3B) enabled a clear, unsupervised clustering of the samples into two groups—tumors with 12q14 amplification alone and those with 1p32 or 6q23 coamplification—based on the same adipogenesis genes. Together, these data suggest that these undifferentiated tumors are committed to differentiate into adipocytes but that this process is blocked by *JUN* overexpression at an early step, between the induction of *C/EBPα* by *C/EBPβ*.

JUN Overexpression Could Block Adipogenesis by Interfering with C/EBPβ Function

The involvement of JUN in cell proliferation is well documented. It has been shown that JUN regulates the expression and function of cell-cycle regulators: in particular, it upregulates *CCND1*, *EGFR*, *HBEGF*, *CSF2*, and *FGF7* genes and downregulates *TP53*, *CDKN2A*, and *CDKN1A* genes (Fu et al., 1999; Passegue et al., 2001; Passegue and Wagner, 2000; Schreiber et al., 1999; Shaulian et al., 2000; Szabowski et al., 2000; Wisdom et al., 1999; Zenz et al., 2003). Nevertheless, from the Affymetrix data, we could not observe any significant difference in the expression levels of these genes between undifferentiated
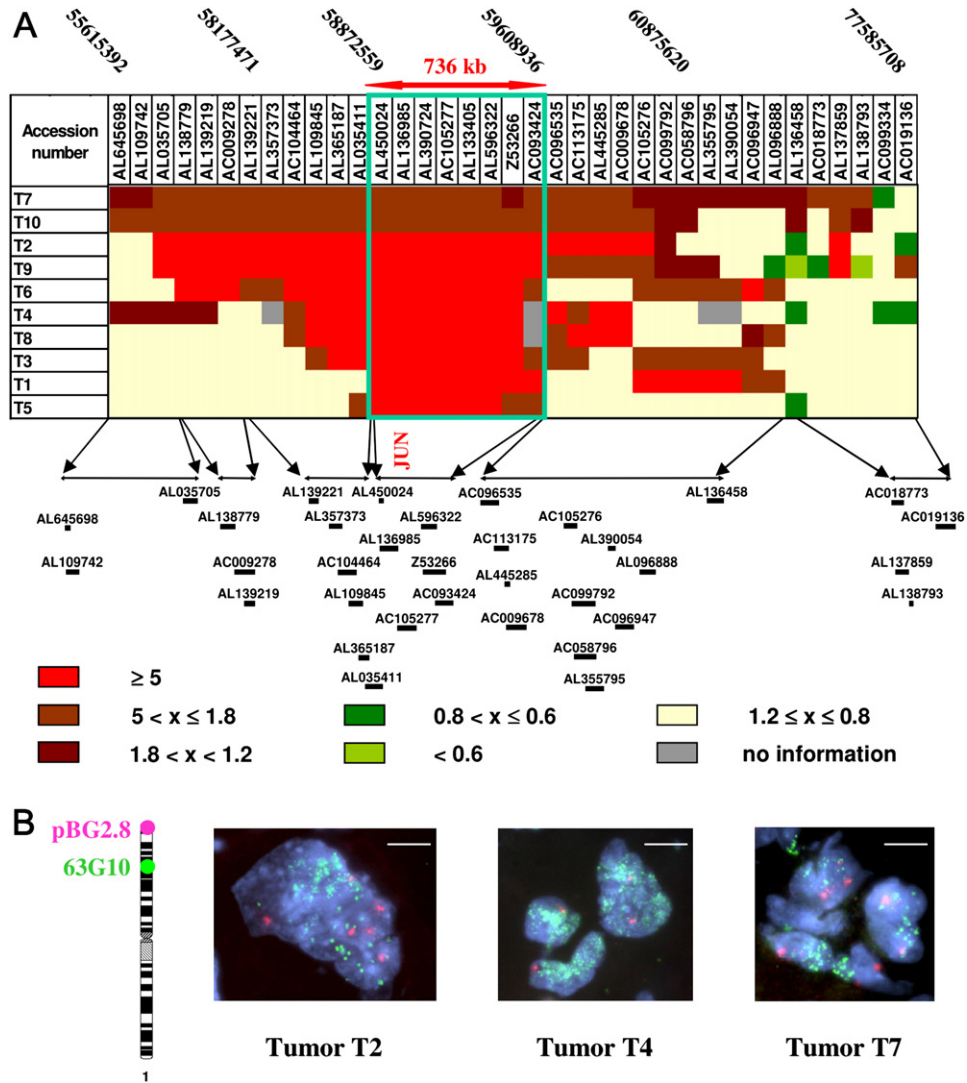
Figure 1. Genomic Amplification of the JUN Locus

(A) The dedicated CGH array contains DNA from 37 BAC-PAC clones corresponding to 1p32 loci. The accession numbers of these clones, as well as their genomic locations, are indicated at the top and at the bottom, respectively. The genomic status (ratio tumor DNA/normal DNA) of each tumor (T1–T10) for each locus is indicated by a color code in filled squares, as defined at the bottom. The location of *JUN* is indicated, as well as the minimal common region of amplification (open green box).

(B) FISH on frozen sections of tumors T2, T4, and T7. The control locus, corresponding to the telomeric locus D1Z2 on the short arm of chromosome 1, is labeled in red (probe pBG2.8, kindly provided by Dr. P. Ambros). The *JUN* probe corresponds to the BAC RP11-63G10 (AL136985); genomic amplification of this locus is observed in all samples. Scale bar, 20 μm.

sarcomas with *JUN* overexpression and well-differentiated tumors (Figure 4A). This observation suggests that the lack of differentiation is not the consequence of a direct induction by JUN of the cell cycle. However, it has been previously shown that JUN can directly interact with C/EBPβ and modulate transcription of its target genes (Hsu et al., 1994; Zagariya et al., 1998). It has also been demonstrated that, in myxoid liposarcomas, the TLS-CHOP oncoprotein prevents adipocyte differentiation by interfering with C/EBPβ (Adelmant et al., 1998; Ron and Habener, 1992). Moreover, a recent report showed that overexpression of DeltaFosB—one of the potential partners of JUN in

the AP-1 transcription complex—decreases adipogenesis in cellular models by interfering with C/EBPβ function, in particular by inhibiting the induction of *C/EBPα* (Sabatakos et al., 2000). As tumors with *JUN* overexpression are blocked between the induction of *C/EBPα* by *C/EBPβ*, we hypothesized that JUN could block adipogenesis by interfering with C/EBPβ. In agreement with this hypothesis, genes directly induced or repressed by C/EBPβ (Akira et al., 1990; Cesi et al., 2005; Christy et al., 1991; Friedman et al., 2004; Jurado et al., 2002; Oishi et al., 2005; Poli et al., 1990; Sebastian et al., 2005; Tang et al., 2004; Umayahara et al., 2002; Wu, 2003; Zauberman
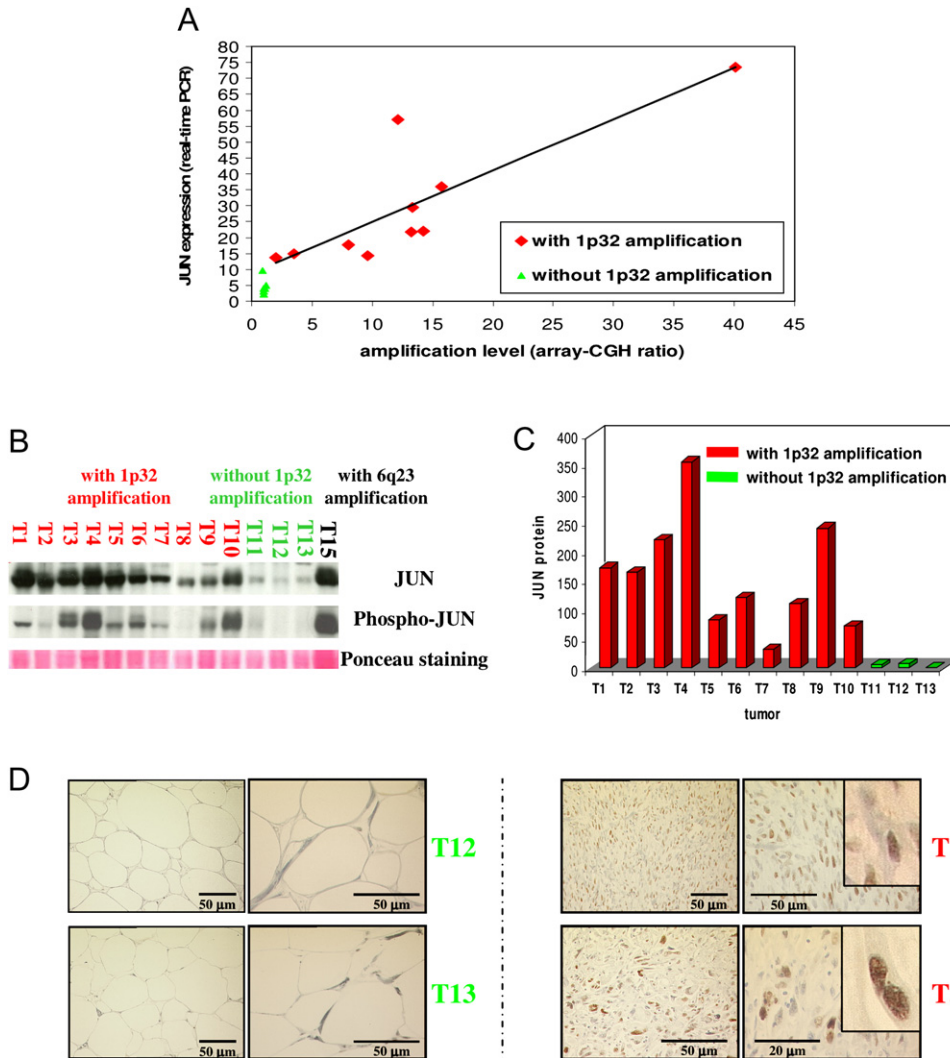
Figure 2. Overexpression of JUN mRNA and Protein

(A) Relative expression levels of *JUN* estimated by real-time PCR (in comparison to well-differentiated liposarcomas) correlate with the genomic amplification level obtained by array CGH experiments.

(B) Immunoblotting of total protein extracts revealed by an anti-JUN antibody, and by an anti-phospho-JUN antibody. Ponceau staining is shown at the bottom as a control for loading. Tumors with *JUN* locus amplification are indicated in red and T15 with 6q23 amplification in black. Three well-differentiated tumors without *JUN* locus amplification are indicated in green.

(C) JUN protein levels normalized according to β-ACTIN expression.

(D) JUN immunohistochemistry performed on two well-differentiated liposarcomas (T12 and T13, left panel), and two undifferentiated sarcomas (T1 and T3, right panel). For these tumors, a magnification is shown in an inset.

et al., 2001; Zhu et al., 1995) are effectively down- or upregulated in tumors with *JUN* overexpression, respectively (Figure 4A). Among them, *C/EBPα* and *PPARγ2*, involved in the differentiation process, are downregulated, and *CCNA2* and *PCNA*, involved in the cell cycle, are upregulated. These data suggest that *JUN* overexpression disturbs the C/EBPβ pathway through a direct interaction between JUN and C/EBPβ proteins and could thus block adipogenesis at two levels: by inhibiting key differentiation factors and by activating cell-cycle genes. In order to document this hypothesis, we performed luciferase reporter gene assays in NIH-3T3 cells, by cotransfection of

a *c/ebpβ* expression plasmid (pcDNA3-C/EBPβ), with a promoter reporter construct (pGL2-Id2/E) and with increasing amounts of a *jun* expression plasmid (RSV-jun). As shown in Figure 4B, luciferase activity regularly decreases when *jun* expression increases, demonstrating that *Id2* promoter induction by *c/ebpβ* is disturbed by Jun protein surexpression. It is noticeable that, whatever the *jun* surexpression level, there is no variation of c/ebpβ protein, and that for 1.25 μg of *jun* expression vector, luciferase activity is similar to that observed when no *c/ebpβ* expression vector is cotransfected. This result strongly suggests that a high level of Jun protein could disturb
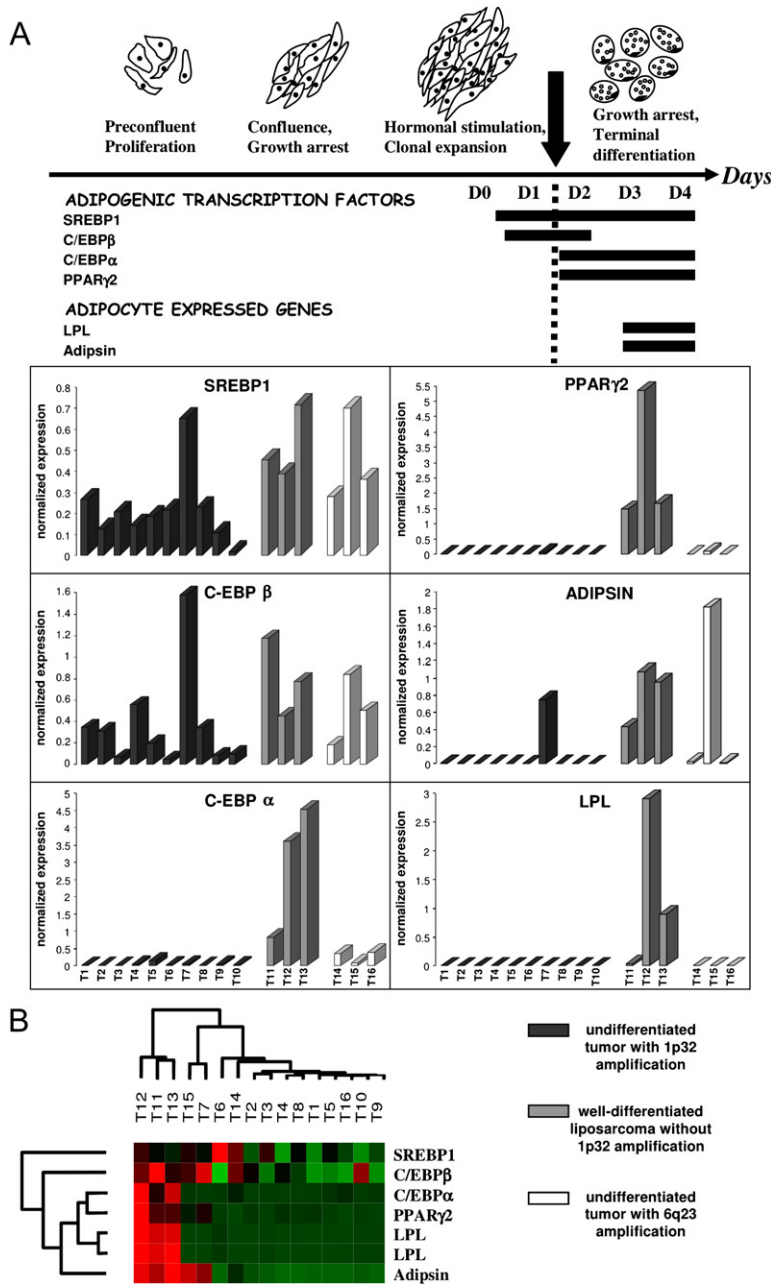
Figure 3. Expression Levels of the Main Adipogenesis Genes in Undifferentiated and Well-Differentiated Tumors

(A) Progression of adipocyte differentiation steps, as well as expression timing of adipogenesis genes, is indicated at the top (adapted from Cowherd et al., 1999). The various gene expression levels were normalized as explained in the Experimental Procedures. The tumor sample numbers are indicated on the x axis.

(B) Affymetrix data obtained for the same set of genes were clustered with the use of the DChip software (average Euclidian algorithm).

expression of *c/ebpβ* target genes, probably titrating c/ebpβ protein by direct interaction.

The 3T3-L1 Cell Line Exhibits Chromosomal Features Close to Those of Liposarcomas

As we could not establish cell lines from well-differentiated or undifferentiated human liposarcomas, we chose to develop a mouse model of liposarcomas by using the murine 3T3-L1 cell line, a preadipocytic nontumoral cell line that has often been used to define molecular events associated with adipogenesis (Cowherd et al., 1999; Green and Kehinde, 1975; Green and Kehinde, 1976; Green and Meuth, 1974; Kim and Spiegelman, 1996; Shao and Lazar,

1997; Yeh et al., 1995) and for which an *mdm2* amplification has been reported previously (Berberich et al., 1999). To delineate more accurately the genomic profile of this cell line, we performed its CGH analysis on a homemade genome-wide mouse BAC array. Strikingly, beside the *mdm2* amplification, we detected high-level amplification of the *cdk6* locus as well as slight amplification of the *jun* locus (Figure 5A). This observation prompted us to verify by FISH these genomic amplifications. As shown in Figure 5B, *mdm2* and *cdk6* loci were coamplified on marker chromosomes or double-minute chromosomes in all the cells analyzed. Most of them did not exhibit *jun* amplification. By contrast, around 1% of the cells harbored
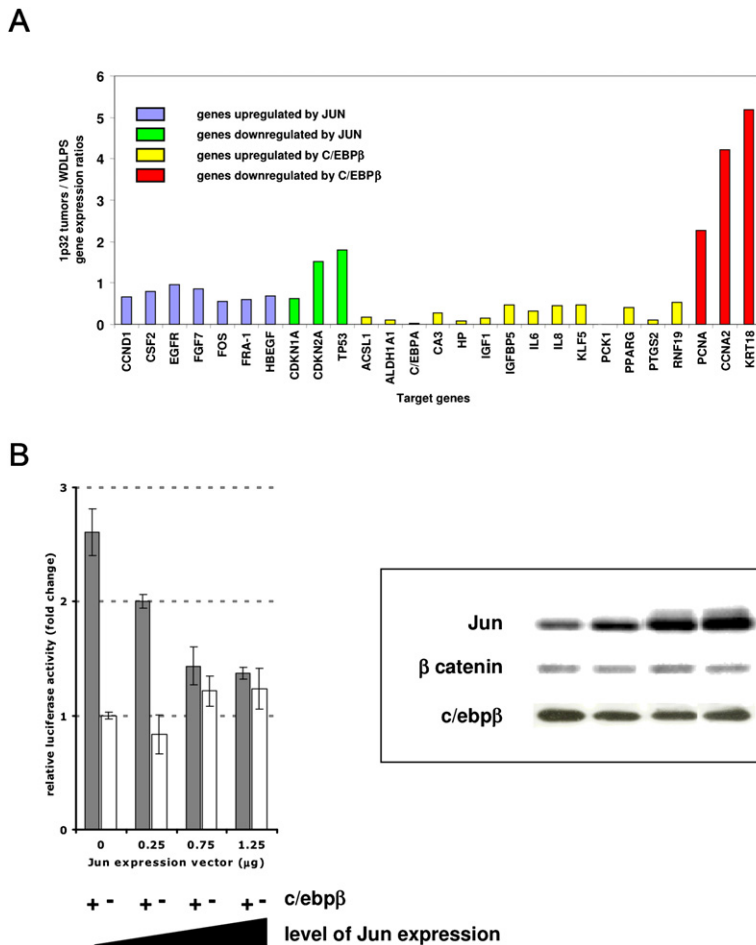
A

B

Figure 4. *JUN* and *C/EBPβ* Target Genes

(A) Expression levels of JUN and C/EBPβ target genes, in 1p32 tumors compared to well-differentiated liposarcomas. For each target gene, the absolute normalized expression values were obtained on Human Genome U133 Plus 2.0 Affymetrix chips (mean of the corresponding probe sets values). The relative expression of these genes in 1p32 tumors versus WDLPS was calculated (ratios between the mean values observed in the two groups of tumors). JUN target genes expression levels are not significantly different (ratios between 0.55 and 1.8), while most C/EBPβ target genes expression levels are highly modified (ratios below 0.54 for the genes upregulated by C/EBPβ, and ratios greater than 2.3 for the genes downregulated by C/EBPβ).

(B) Luciferase c/ebpβ reporter assay. Luciferase activity is shown (mean of independent duplicates ± SD), in relation with increasing amounts of *jun* expression vector. Gray and white boxes correspond to luciferase activity, in the presence or absence of *c/ebpβ* expression vector, respectively. All results correspond to fold change induction, compared to the basal luciferase activity in cells transfected with the luciferase construct only. In the presence of *c/ebpβ* expression vector, a clear and regular decrease of luciferase activity is observed when *jun* expression increases. Western blots on the right, corresponding to the gray boxes conditions, show that jun protein expression increases without any modification of the c/ebpβ protein level (Anti-c/ebpβ abcam ab15050, dilution: 1/1000).

a high-level amplification of *jun* on double-minute or marker chromosomes (Figure 5C). As noted above, well-differentiated human liposarcomas are characterized by amplifications and overexpressions of *MDM2* and *CDK4* genes. CDK4 and CDK6 are closely related proteins that play similar roles in cell-cycle progression by phosphorylating RB1. Despite the fact that the 3T3-L1 cell line is not derived from a mouse tumor, it appears to be a highly relevant cellular model of human liposarcoma.

3T3-L1 Cells Induce Liposarcoma-Like Tumors in Nude Mice

It has been previously described that injection of 3T3-L1 and 3T3-F442A (another preadipocyte cell line) cells into nude mice led to the development of flattened fat pads (Fischbach et al., 2004; Green and Kehinde, 1979; Neels et al., 2004). We injected 3×10^6, 6×10^6, and 10×10^6 3T3-L1 cells subcutaneously into the flank of athymic female nude mice (two mice for each experimental condition).

Four weeks after injection, we observed small subcutaneous tumors in all mice. These tumors grew progressively, looking like the flattened fat pads previously described. Finally, the tumors became more prominent,

firmer, and much more vascular (Figure 6A). Two tumors were removed at an early stage (fat-pad stage), two at an intermediate stage, and two at a later stage (firm and vascular stage). Macroscopic examination revealed that most of these tumors contained different areas of more or less firm tissue. Histopathological analysis showed two components: a well-differentiated liposarcoma area (preponderant at the fat-pad stage), and an undifferentiated area (preponderant at the late stage) (Figure 6B).

Immunohistochemistry revealed that the undifferentiated area was strongly positive for Jun expression, whereas the well-differentiated areas were negative (Figure 6C). This suggested that the undifferentiated component might be derived from the cells with high-level amplification of *jun* described above in the wild-type 3T3-L1 cell line.

To verify this hypothesis, we performed a FISH analysis of frozen and paraffin-embedded sections of the mouse tumors. High-level amplification of *jun* was observed in large nuclei from the undifferentiated areas of the tumors (Figures 7A, 7B, and 7D), but not in nuclei from the well-differentiated areas (Figures 7B and 7C), which exhibit only *mdm2* and *cdk6* loci amplification. Short-term cultures were performed on one undifferentiated mouse tumor,
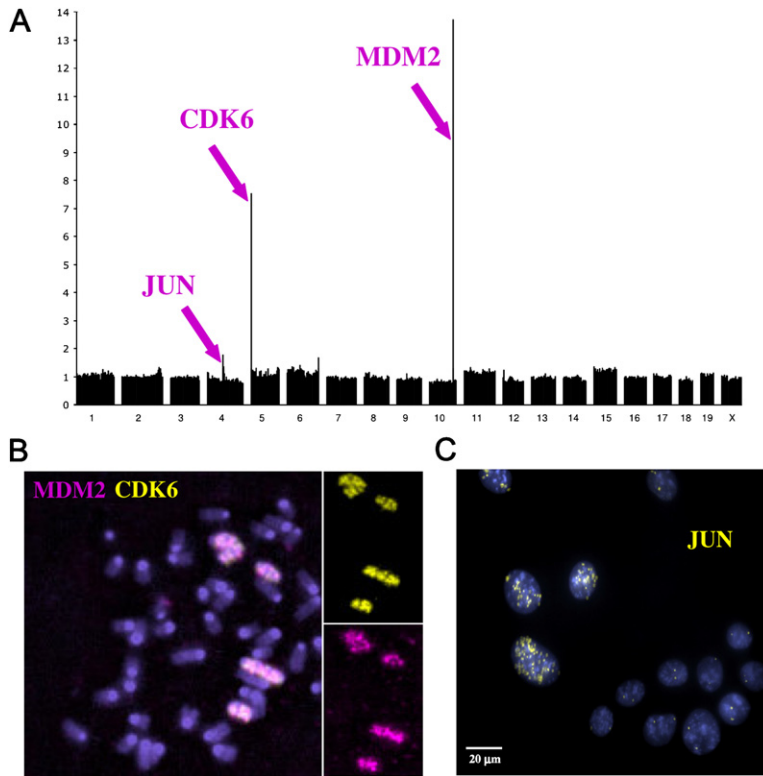
Figure 5. Genomic Profile of the 3T3-L1 Cell Line

(A) CGH array profile of 3T3-L1 cell line obtained on a home-made mouse array. Loci corresponding to *jun*, *cdk6*, and *mdm2* are indicated. Chromosome numbers, x axis; DNA ratios, y axis.

(B) Dual-color FISH on a 3T3-L1 metaphase. The *cdk6* probe is labeled in yellow, and the *mdm2* probe is labeled in pink. Single-color images of the same mitosis are shown on the right.

(C) High-level amplification of the *jun* locus (yellow) can be observed by FISH in a small percentage of nuclei.

and metaphase spreads were obtained. FISH analysis demonstrated a high-level genomic amplification of the *jun* locus in all cells (Figure 7E). *Jun* overexpression was also confirmed by real-time PCR in all tumors; expression was increased 16-fold, as a mean, compared to wild-type 3T3-L1 cells.
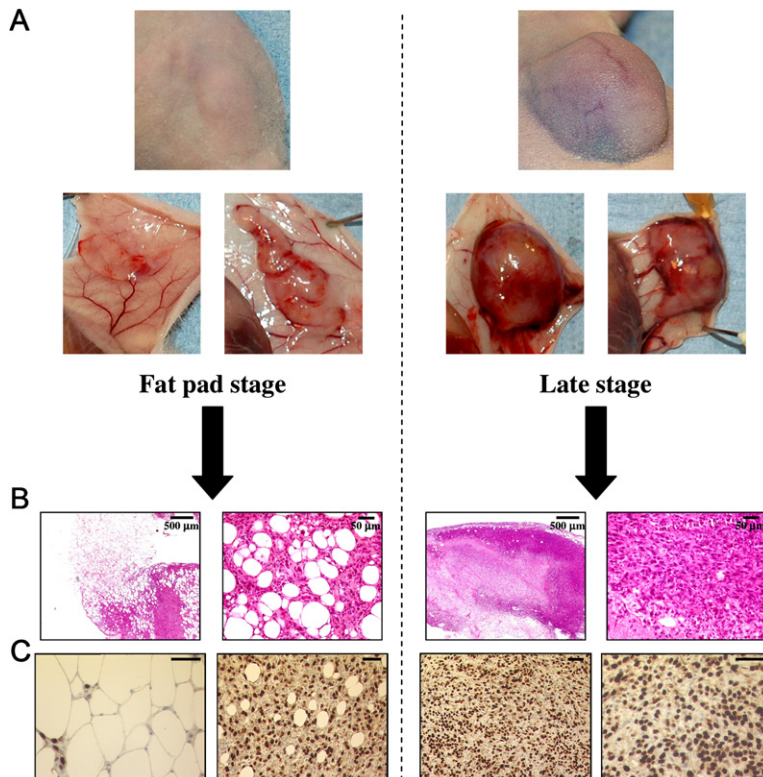

Figure 6. Tumors Obtained after 3T3-L1 Injection in Nude Mice

(A) Representative tumors are shown at early (left) and late (right) stages after 3T3-L1 cells injection into nude mice.

(B) Histopathology reveals the presence of two components in fat-pad tumors. The main part of the tumors corresponds to a well-differentiated adipose tissue, infiltrated by undifferentiated cells. In late stage tumors, almost all the cells are undifferentiated. For each stage, two magnifications are shown.

(C) In fat-pad tumors, immunohistochemistry reveals a strong Jun labeling in the undifferentiated component (right), whereas well-differentiated areas (left) were Jun negative. In late-stage tumors, the main part of the tumor appears uniformly undifferentiated and positive for Jun (two magnifications are shown). Scale bar, 50 μm.
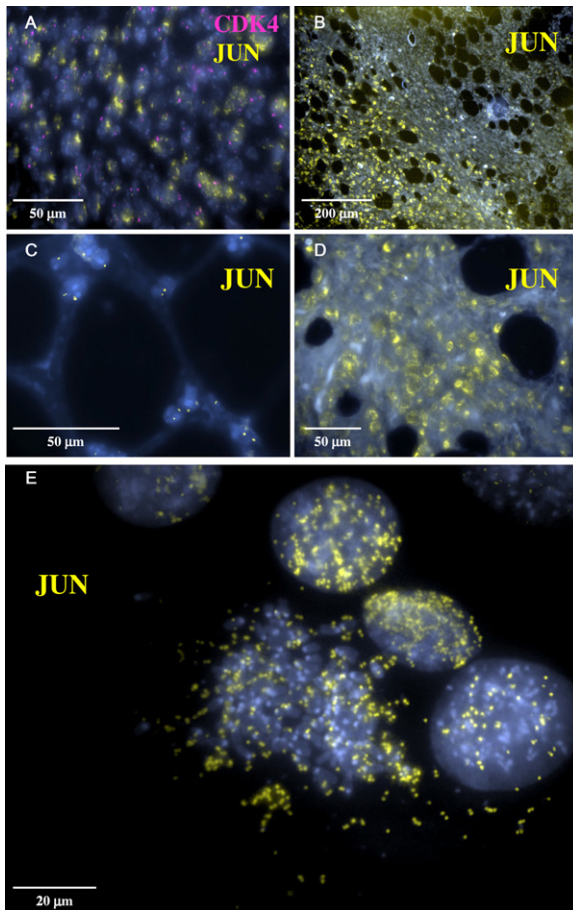
Figure 7. FISH Experiments Performed on Tumors Obtained after 3T3-L1 Cell Injection into Nude Mice

(A) Frozen tissue section from an undifferentiated tumor. The *jun* locus, labeled in yellow, is highly amplified. The *cdk4* locus, labeled in pink, is a ploidy control locus, not amplified in the tumor.

(B) *jun* hybridization on a paraffin-embedded tissue section from a tumor with well-differentiated area (right side), and undifferentiated area (left side). The *jun* locus is amplified only in the undifferentiated area.

(C) Focus on the well-differentiated area from the same tumor as in (B), with two *jun* loci in each nucleus.

(D) Focus on the undifferentiated area from the same tumor as in (B), exhibiting high-level amplification of the *jun* locus in all nuclei.

(E) Short-term culture obtained from an undifferentiated late tumor. One metaphase (left) and nuclei are shown. *Jun* locus is labeled in yellow. High-level amplification of *jun* as double-minute chromosomes is observed in metaphase and interphase nuclei.

These findings are in good agreement with the other data presented above. They suggest that the 3T3-L1 cells harboring high-level amplification of *jun* are selected in vivo, and that they are associated with a more proliferative and undifferentiated status. One cell line, LM3D, was established from a late-stage mouse tumor. FISH analysis of this cell line reveals a constant high-level amplification of the *jun* locus. LM3D cell growth in vitro was compared to that of the 3T3-L1 cell line. As shown in Figure 8A, the proliferation rate was slightly lower for LM3D than for

3T3-L1, suggesting that the aggressiveness of LM3D-induced tumors is not directly the consequence of a high proliferation rate. In marked contrast with this anchorage-dependent proliferation, LM3D cells grown in soft agar form more numerous, larger, and more invasive colonies than 3T3-L1 cells (Figure 8B). This suggests that LM3D cells are associated with a tumorigenicity higher than that of 3T3-L1 cells, a feature that could be a consequence of *jun* overexpression, as recently described in human lung cancers (Maeno et al., 2006).

When grown to confluence and treated with "differentiating medium" as previously described (Student et al., 1980; Yeh et al., 1995), this cell line does not exhibit a terminal adipocytic differentiation after oil red O stain (a specific lipid stain), contrary to the 3T3-L1 cell line grown in the same conditions (Figure 8C). According to the hypothesis that *JUN* overexpression blocks adipogenesis by interfering with C/EBPβ function and as observed in human tumors, the differentiation process of LM3D, analyzed by real-time PCR, is blocked before the induction of C/EBPα (Figure 8D).

We then injected 6×10^6 LM3D cells to nude mice and 6×10^6 3T3-L1 cells to control mice. Three weeks after injection, and contrary to control mice, which do not present any sign of tumor development, all mice injected with LM3D cells develop firm, vascular, and highly proliferative tumors without any evidence of differentiation at histopathological analysis. All the cells from these tumors were strongly positive for Jun expression (data not shown).

Overexpression of *jun* in 3T3-L1 Cells Delays Its Inducible Adipocytic Differentiation

We then transfected a vector expressing *jun* into 3T3-L1 cells. A clone overexpressing *jun* (A3JUN), a control clone containing the empty vector (A1CT), and wild-type 3T3-L1 cells were grown to confluence and then treated with "differentiating medium." We confirmed by FISH that the A3JUN clone was established from a 3T3-L1 cell without endogenous *Jun* amplification (data not shown). As early as the second day after induction, massive adipocyte differentiation was observed by oil red O stain in the A1CT control clone and in 3T3-L1 wild-type cells, whereas no labeling was detected at this stage in A3JUN cells (Figure 8E). When maintained for a further 4 days at confluence in differentiating medium, the A3JUN cells began to slightly differentiate (Figure 8E), suggesting that adipocyte differentiation was blocked or largely delayed in this clone.

Role of JUN in Oncogenesis and Differentiation

JUN oncoprotein plays multiple roles at the interface between cell proliferation and differentiation. *Jun* overexpression is not oncogenic alone in transgenic mice (Grigoriadis et al., 1993); nevertheless, its viral homolog *v-Jun* induces fibrosarcomas in chicken (Cavalieri et al., 1985; Maki et al., 1987) and wound-induced tumors in transgenic mice (Schuh et al., 1990). In human, *JUN* overexpression without a concomitant increase of its
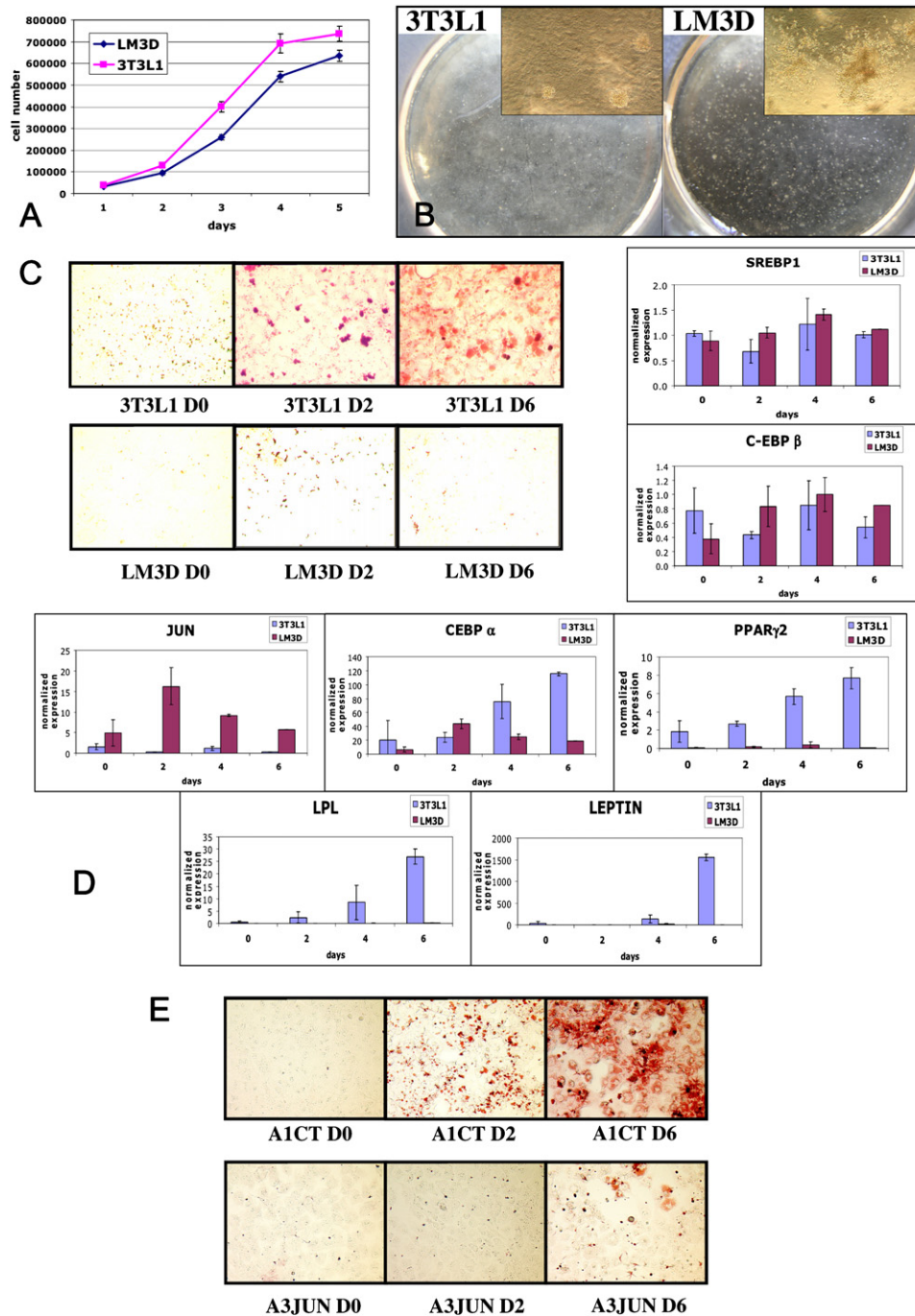
Figure 8. Differentiation of Adipocyte Cell Lines In Vitro

(A) LM3D cell line, established from a late-stage mouse tumor, was grown in parallel to 3T3-L1 cells, and their growth was assessed over a 5 day time course (mean of triplicates ± SD).

(B) LM3D cells (overexpressing *jun*) and 3T3-L1 cells were plated in soft-agar assays and allowed to grow for 4 weeks. Colonies were two times more numerous, larger, and irregular in LM3D wells. The insets show a magnification of the colonies.

(C) LM3D cell line was grown to confluence and treated with differentiating medium. This cell line (bottom) does not exhibit adipocytic differentiation (oil red O staining) after 6 days of treatment (D6), contrary to the 3T3-L1 cell line (top).

(D) Expression levels of *jun* and of the main adipogenesis genes in 3T3-L1 and LM3D cell lines (mean of independent duplicates, ± SD). In LM3D cell line, adipogenesis process is blocked before the induction of C/EBPα by C/EBPβ, as observed in human tumors.

(E) The A1CT control clone (top) is transfected with empty vector. Its differentiation into adipocytes (oil red O staining) starts 2 days (D2) after stimulation by the differentiating treatment. In the A3JUN clone (bottom), which is transfected with the vector expressing *jun*, differentiation is delayed, starting only at day 6 (D6).

phosphorylation has been described in some tumors (Mathas et al., 2002; Rangatia et al., 2003). In these tumors, as well as in undifferentiated liposarcomas, enhanced JUN transcription activity may be the consequence of titration of its repressor complex by an increase in JUN protein level, as recently suggested (Weiss and Bohmann, 2004). Furthermore, it has been recently described that intestinal tumorigenesis is increased by c-Jun phosphorylation (Nateri et al., 2005). It has also been demonstrated that Jun stimulates angiogenesis, through proliferin activation, in a cell model of fibrosarcoma (Toft et al., 2001).

The data provided here demonstrate that amplification and overexpression of *JUN* block adipocytic differentiation at an early step and is associated with a much more aggressive phenotype in corresponding tumors. In human sarcomas, its overexpression likely blocks the adipocytic differentiation of human liposarcomas with 12q14 amplification, leading to more aggressive undifferentiated tumors. To our knowledge, *JUN* amplification has not previously been described in a human tumor (Jochum et al., 2001; Vogt, 2001). Only few data on the role of JNK-JUN pathway activation in adipogenesis are available; JNK activation blocks adipogenesis through PPARγ phosphorylation (Adams et al., 1997; Camp and Tafuri, 1997; Camp et al., 1999; Hu et al., 1996). It has also been reported that JNK negatively regulates adipocyte differentiation from human mesenchymal stem cells through CREB downregulation (Tominaga et al., 2005). Nevertheless, other data suggest that JNK1 pathway inactivation could interfere with formation of subcutaneous fat in obese mice, suggesting that JNK1 activation could also, in some instances, accelerate fat deposition (Hirosumi et al., 2002). However, in this mouse model, it is not clear whether the effect is on the adipocyte differentiation or on energy metabolism. Our previous results obtained on sarcomas with amplification/overexpression of MAP3K5, an upstream activator of JNK, are in agreement with a negative role of JNK1 on adipocyte differentiation (Chibon et al., 2004). The present results demonstrate that overexpression of *JUN*, a downstream target of the JNK pathway, leads to a similar negative regulation of adipogenesis. As indicated above, the overexpression of DeltaFosB decreases adipogenesis by interfering with C/EBPβ function (Sabatakos et al., 2000). This feature, which is reminiscent of what we have observed in undifferentiated human liposarcomas and in the mouse LM3D cell line, suggests that *JUN* overexpression might block adipogenesis in human tumors through an interaction with C/EBPβ. Finally, it is also of interest to note that late-stage tumors obtained after 3T3-L1 injection in nude mice appear more vascular, a feature which could be related to the induction of angiogenesis by Jun, as previously described (Toft et al., 2001).

The molecular data presented in this study suggest that, in human sarcomas, *JUN* overexpression could interfere with adipocytic differentiation. The cellular and xenograft models described here would be particularly efficient tools for the analysis of the connections between oncogenesis and differentiation in sarcomas.

EXPERIMENTAL PROCEDURES

Tumor Samples

Tumors T1–T10 and T14–T16 were classified as undifferentiated sarcomas by the pathologists of the French Sarcoma Group. All these tumors were associated with a MIB1 positivity in more than 10% of the cells (range: 10%–70%). All but one were negative for BCL2 labeling. Tumors T11–T13 correspond to well-differentiated liposarcomas. All these WDLPS were positive for MIB1 in less than 5% of the cells, and negative for BCL2 labeling. The mean age of the patients was 65. All tumors except two were localized in retroperitoneum. According to French law at the time of the study, the tumor samples were collected in agreement with the ANAES recommendations. Informed consent was obtained from all patients. Experiments were performed in agreement with the Bioethics Law n° 2004-800, and the Ethics Charter from the National Institute of Cancer (INCa).

Human Array CGH

DNA from BACs (bacterial artificial chromosomes) and PACs (P1-derived artificial chromosomes) were obtained after isolation of one bacterial colony and amplification by Qiagen Plasmid Maxi Kit, using the conditions of low-copy-number plasmids. The genomic location of BACs or PACs was checked by hybridization on normal metaphase spreads. Sonicated BACs and PACs were spotted in duplicate on Corning Ultragaps slides in 75% formamide (37 BACs/PACs located in the 1p32 band, 56 in the 6q23 band, and 29 in the 12q14 band). After rehydration and UV fixation, slides were blocked for 15 min with succinic anhydride/1-methyl 2-pyrrolidinone/sodium borate pH8 solution. Slides were denatured for 2 min in boiling water, dehydrated in 95% ethanol, and dried by centifugation at 400 rpm.

After DpnII digestion (Biolabs) and purification with PCR Purification Kit (Qiagen), 1.5 μg of tumor DNA and 1.5 μg of normal DNA were labeled, respectively, with dCTP-Cy5 or dCTP-Cy3 (Amersham) by random priming (BioPrime DNA Labeling System Kit, Invitrogen). The reaction was performed at 37°C for 3 hr. After purification on microcon YM30 (Millipore) and denaturation at 92°C, these DNAs were prehybridized with 200 μg of Cot-1 DNA (Roche) for 30 min at 37°C in 15 μl of hybridization buffer (50% formamide, 40 mM NaH$_2$PO$_4$, 0.1% SDS, 10% dextran sulfate, 2× SSC, Denhardt's solution) and put on treated microarray slides. After 24 hr hybridization at 37°C, slides were washed for 5 min in 0.5× SSC, 0.03% SDS at 65°C, and for 5 min in 0.5× SSC, 0.03% SDS at 45°C. After drying by centrifugation, slides were read with GenePix 4000B scanner (Axon Instruments). Results were analyzed with GenePix Pro 5.1 software. To normalize data, we used 6q23 spots, which have normal genomic status in these tumors.

Mouse Array CGH

A homemade genome-wide mouse BAC array was built in the laboratory. This array contains 696 BACs that were isolated, validated by end-sequencing, and amplified by multiple displacement amplification. The collection was spotted in quadruplicate in 75% formamide on Corning Ultragaps slides. We used this array in the same way as we used human CGH array, but replacing human Cot-1 by mouse Cot-1 and normal human DNA by normal mouse liver DNA.

FISH on Metaphase Spreads, Frozen Tissue Sections, and Paraffin Sections

Metaphase spreads were obtained by standard procedures. For frozen tissues, 5 μm thick tumor sections were used. Before denaturation, slides were treated for 10 min in 2× SSC and dehydrated in successively increasing concentrations of ethanol (70%, 90%, and 100%), 5 min each. For paraffin sections, slides were treated by the Zymed conversion kit, according to the manufacturer's protocol. BAC and PAC labeling by nick-translation, denaturation, and detection were achieved as previously described (Schleiermacher et al., 2004).

Real-Time PCR

Total tumor RNAs were extracted either from frozen tumor samples or from cell lines by Trizol extraction (Life Technologies, Inc., Rockville, MD). To eliminate DNA contamination, RNAs were treated with RNase-free DnaseI (Roche): 3 μg of RNA was treated with 10 U of DNase in DNase buffer (Invitrogen). The reaction was performed at 37°C for 30 min and stopped by the addition of 1 μl of 25 mM EDTA and heating for 10 min at 65°C. The RNA was reverse transcribed into cDNA with the GeneAmp RNA PCR Core Kit (Applied Biosystems). Real-time PCR was performed with SYBR Green Master Mix (Applied Biosystems). Human *JUN* primers were previously described (Jean et al., 2001). Forward and reverse primers were as follows: 5′-CACGTTAA CAGTGGGTGCCA-3′ and 5′-CCCCGACGGTCTCTCTTCA-3′ for human *JUN*; 5′-CTTCAACAGCGACACCCACT-3′ and 5′-GTGGTCCA GGGGTCTTACTC-3′ for human *GAPDH*; 5′-AACGCCATTGAGAAG CGCTA-3′ and 5′-GCAAGACAGCAGATTTATTCAG-3′ for human *SREBP1*; 5′-CAGGTCAAGAGCAAGGCCAA-3′ and 5′-CGCACGGC GATGTTGTTGC-3′ for human *C-EBPβ*; 5′-GACCTAGAGATCTGGCT GTG-3′ and 5′-GATGGACTGATCGTGCTTCG-3′ for human *C-EBPα*; 5′-CTGTCTGCAAACATATCACAAG-3′ and 5′-GGAGTGGTCTTC CATTACGG-3′ for human *PPARγ2*; 5′-ATCACCGAGCGCTTGAT GTG-3′ and 5′-CTTCTTGCGGTTGCCGCAAA-3′ for human *ADIPSIN*; 5′-GGACAATGTCCATCTCTTGG-3′ and 5′-GTAAGACGTCTACAAAA TCTGC-3′ for human *LPL*; 5′-AGTCATGAACCACGTTAACAG-3′ and 5′-AGCCCTGACAGTCTGTTCTC-3′ for murine *jun*; 5′-AAAATGGTG AAGGTCGGTGT-3′ and 5′-TGACTGTGCCGTTGAATTTG-3′ for murine *gapdh*; 5′-AGAAGCGCACAGCCCACAAT-3′ and 5′-GCAAGACA GCAGATTTATTCAG-3′ for murine *srebp1*; 5′-CCAAGGCCAAGGCC AAGAAG-3′ and 5′-TGCGCACCGCGATGTTGTTG-3′ for murine *c-ebpβ*; 5′-AGTCGGTGGACAAGAACAGC-3′ and 5′-ACTCCAGCACCT TCTGTTGC-3′ for murine *c-ebpα*; 5′-GCTGTTATGGGTGAAACTCT-3′ and 5′-TGGCATCTCTGTGTCAACCA-3′ for murine *pparγ2*; 5′-CGGG GTAGTCACCATTAACA-3′ and 5′-CTTTTTGCCATTGCCACAGA-3′ for murine *adipsin*; 5′-TAGACAACGTCCACCTCTTAG-3′ and 5′-GTAAGACATCTACAAAATCAGC-3′ for murine *lpl*; 5′-CAATGACAT TTCACACACGCAG-3′ and 5′-GCTGGTGAGGACCTGTTGAT-3′ for murine *leptin*.

All the real-time PCR annealing and extension were performed at 60°C. Each reaction was performed in duplicate.

To normalize the data, we used the *GAPDH* genes as reference genes. Human tumor data were normalized against an RNA pool of two well-differentiated liposarcomas in which the *JUN* expression level is basal. For murine cell-line analyses, data were normalized against wild-type 3T3-L1 at day 0 before addition of the differentiating medium. The results were calculated as previously described (De Preter et al., 2002).

Western Blot

Total proteins were extracted by crushing frozen tumor samples in 2× Laemmli buffer. Extracts were probed with a primary anti-c-JUN antibody (H79) (Santa Cruz Biotechnology) or anti-β-actin antibody (Sigma-Aldrich) at a dilution of 1:500 and 1:10,000, respectively. Anti-phospho-jun antibody was kindly provided by F. Mechta-Grigoriou (Lallemand et al., 1998) and used at a dilution of 1:200. Anti-SAPK/JNK and phospho-SAPK/JNK (Cell Signaling) were used at a dilution of 1:200. The secondary antibodies were horseradish peroxidase-conjugated anti-rabbit or anti-mouse (APBiotech), as appropriate, and the signal was detected by enhanced chemiluminescence (SuperSignal West Pico Chemiluminescent substrate, Pierce). Western blot images were acquired with a FUJIFILM luminescent image LAS-1000plus analyzer. They were analyzed with Image Gauge v 4.0 software, which allowed us to normalize JUN expression data to β-actin expression values.

Immunohistochemistry

Immunohistochemistry was performed in all cases on a representative paraffin block with anti-JUN antibody (H79) at a dilution of 1:1000, according to the method described previously (Coindre et al., 2003).

Transcriptome Analysis

RNA quality was checked on an Agilent 2100 bioanalyzer (Agilent Technologies). Samples were then analyzed on Human Genome U133 Plus 2.0 chip (Affymetrix), according to the manufacturer's procedures. Data were normalized using the DChip software.

Reporter Gene Assay

Experiments were performed twice on NIH-3T3 cells. Briefly, 10^5 cells were seeded in duplicate in 12-well plates in DMEM (Gibco) plus 10% fetal bovine serum (Gibco). One day later, 50 ng of a *c/ebpβ* expression plasmid (pcDNA3-C/EBPβ [Zhu et al., 2002]), 750 ng of a promoter reporter construct containing part of the c/ebpβ responsive *Id2* gene fused with the luciferase gene (pGL2-Id2/E [Karaya et al., 2005]), increasing amounts (from 250 to 1250 ng) of a *jun* expression plasmid (RSV-jun; Pfarr et al., 1994), and 5 ng of pRL-SV40 *Renilla* luciferase control were transfected in each well, with Effecten transfection reagents (Qiagen). The total amount of DNA among all conditions was kept constant by adding RSV-βgal plasmid DNA. Using the Dual-Luciferase reporter assay system (Promega), total cell lysates were prepared 48 hr after transfection, and luciferase assays were performed according to the manufacturer's instructions.

Tumor Xenografts

We injected $3 × 10^6$, $6 × 10^6$, and $10 × 10^6$ native 3T3-L1 cells subcutaneously into the flank of 8-week-old athymic female nude mice (two mice for each experimental condition). Two mice were sacrificed at an early stage, two were sacrificed at an intermediate stage, and two were sacrificed at a late stage. For each case, we froze and studied independently tumor fragments with macroscopically different appearances. All the tumors were analyzed by CGH-array, FISH, and immunohistochemistry. Experiments were performed in accordance with relevant institutional guidelines from the Direction Départementale des Services Vétérinaires de Paris (approval B750518).

Preparation of a Stable Cell Line

The 3T3-L1 cell line was graciously provided by B. Feve (Mercier et al., 2001). 3T3-L1 cells were seeded at a density of $4.3 × 10^5$ per 10 cm diameter culture dish in DMEM (Gibco) plus 10% donor calf serum (Gibco). After 48 hr, cells were transfected with 10 μg of plasmid overexpressing *jun*, or of a control plasmid, in the presence of 30 μl of Lipofectamine (Invitrogen). These plasmids were generously provided by F. Mechta-Grigoriou (Pfarr et al., 1994). In the plasmid overexpressing *jun*, the murine *jun* cDNA is cloned downstream of the Moloney murine leukemia virus long terminal repeat and the *neo*^{r} selection gene downstream of the metallothionein promoter. The control plasmid contains only the Moloney murine leukemia virus long terminal repeat and the *neo*^{r} selection gene downstream of the metallothionein promoter. After 24 hr, 800 μg/ml G418 was added to the medium. Individual clones were picked and characterized by real-time PCR.

Oil Red O Staining

After three washes in 1× PBS, cells were fixed with 3.7% formaldehyde (Sigma) for 5 min at room temperature. After a second wash, cells were stained with a filtered solution of 0.3% oil red O for 30–40 min. Finally, cells were washed three times with water.

Proliferation and Soft-Agar Assays

For proliferation rate assays, $2 × 10^4$ cells were seeded in 24-well plates in DMEM (Gibco) plus 10% donor calf serum (Gibco). Cells from triplicates were counted every day with a Z2 Coulter counter (Beckman Coulter).

Soft-agar assays were performed in duplicates. For these assays, $1 × 10^4$ cells were added to 1 ml of growth medium with 0.3% agar and layered onto 1 ml of 0.3% agar beds in 6-well plates. Colonies were photographed and counted in four independent wells.

REFERENCES

Adams, M., Reginato, M.J., Shao, D., Lazar, M.A., and Chatterjee, V.K. (1997). Transcriptional activation by peroxisome proliferator-activated receptor gamma is inhibited by phosphorylation at a consensus mitogen-activated protein kinase site. J. Biol. Chem. *272*, 5128–5132.

Adelmant, G., Gilbert, J.D., and Freytag, S.O. (1998). Human translocation liposarcoma-CCAAT/enhancer binding protein (C/EBP) homologous protein (TLS-CHOP) oncoprotein prevents adipocyte differentiation by directly interfering with C/EBPbeta function. J. Biol. Chem. *273*, 15574–15581.

Akira, S., Isshiki, H., Sugita, T., Tanabe, O., Kinoshita, S., Nishio, Y., Nakajima, T., Hirano, T., and Kishimoto, T. (1990). A nuclear factor for IL-6 expression (NF-IL6) is a member of a C/EBP family. EMBO J. *9*, 1897–1906.

Angel, P., Allegretto, E.A., Okino, S.T., Hattori, K., Boyle, W.J., Hunter, T., and Karin, M. (1988). Oncogene jun encodes a sequence-specific trans-activator similar to AP-1. Nature *332*, 166–171.

Berberich, S.J., Litteral, V., Mayo, L.D., Tabesh, D., and Morris, D. (1999). mdm-2 gene amplification in 3T3-L1 preadipocytes. Differentiation *64*, 205–212.

Bohmann, D., Bos, T.J., Admon, A., Nishimura, T., Vogt, P.K., and Tjian, R. (1987). Human proto-oncogene c-jun encodes a DNA binding protein with structural and functional properties of transcription factor AP-1. Science *238*, 1386–1392.

Camp, H.S., and Tafuri, S.R. (1997). Regulation of peroxisome proliferator-activated receptor gamma activity by mitogen-activated protein kinase. J. Biol. Chem. *272*, 10811–10816.

Camp, H.S., Tafuri, S.R., and Leff, T. (1999). c-Jun N-terminal kinase phosphorylates peroxisome proliferator-activated receptor-gamma1 and negatively regulates its transcriptional activity. Endocrinology *140*, 392–397.

Cavalieri, F., Ruscio, T., Tinoco, R., Benedict, S., Davis, C., and Vogt, P.K. (1985). Isolation of three new avian sarcoma viruses: ASV *9*, ASV *17*, and ASV 25. Virology *143*, 680–683.

Cesi, V., Giuffrida, M.L., Vitali, R., Tanno, B., Mancini, C., Calabretta, B., and Raschella, G. (2005). C/EBP alpha and beta mimic retinoic acid activation of IGFBP-5 in neuroblastoma cells by a mechanism independent from binding to their site. Exp. Cell Res. *305*, 179–189.

Chibon, F., Mariani, O., Derre, J., Malinge, S., Coindre, J.M., Guillou, L., Lagace, R., and Aurias, A. (2002). A subgroup of malignant fibrous histiocytomas is associated with genetic changes similar to those of well-differentiated liposarcomas. Cancer Genet. Cytogenet. *139*, 24–29.

Chibon, F., Mariani, O., Derre, J., Mairal, A., Coindre, J.M., Guillou, L., Sastre, X., Pedeutour, F., and Aurias, A. (2004). ASK1 (MAP3K5) as a potential therapeutic target in malignant fibrous histiocytomas with 12q14-q15 and 6q23 amplifications. Genes Chromosomes Cancer *40*, 32–37.

Christy, R.J., Kaestner, K.H., Geiman, D.E., and Lane, M.D. (1991). CCAAT/enhancer binding protein gene promoter: Binding of nuclear factors during differentiation of 3T3–L1 preadipocytes. Proc. Natl. Acad. Sci. USA *88*, 2593–2597.

Coindre, J.M., Mariani, O., Chibon, F., Mairal, A., De Saint Aubain Somerhausen, N., Favre-Guillevin, E., Bui, N.B., Stoeckle, E., Hostein, I., and Aurias, A. (2003). Most malignant fibrous histiocytomas developed in the retroperitoneum are dedifferentiated liposarcomas: A review of 25 cases initially diagnosed as malignant fibrous histiocytoma. Mod. Pathol. *16*, 256–262.

Cowherd, R.M., Lyle, R.E., and McGehee, R.E., Jr. (1999). Molecular regulation of adipocyte differentiation. Semin. Cell Dev. Biol. *10*, 3–10.

De Preter, K., Speleman, F., Combaret, V., Lunec, J., Laureys, G., Eussen, B.H., Francotte, N., Board, J., Pearson, A.D., De Paepe, A., et al. (2002). Quantification of MYCN, DDX1, and NAG gene copy number in neuroblastoma using a real-time quantitative PCR assay. Mod. Pathol. *15*, 159–166.

Fischbach, C., Spruss, T., Weiser, B., Neubauer, M., Becker, C., Hacker, M., Gopferich, A., and Blunk, T. (2004). Generation of mature fat pads in vitro and in vivo utilizing 3-D long-term culture of 3T3–L1 preadipocytes. Exp. Cell Res. *300*, 54–64.

Forus, A., Florenes, V.A., Maelandsmo, G.M., Meltzer, P.S., Fodstad, O., and Myklebost, O. (1993). Mapping of amplification units in the q13–14 region of chromosome 12 in human sarcomas: Some amplica do not include MDM2. Cell Growth Differ. *4*, 1065–1070.

Friedman, J.R., Larris, B., Le, P.P., Peiris, T.H., Arsenlis, A., Schug, J., Tobias, J.W., Kaestner, K.H., and Greenbaum, L.E. (2004). Orthogonal analysis of C/EBPbeta targets in vivo during liver proliferation. Proc. Natl. Acad. Sci. USA *101*, 12986–12991.

Fu, S., Bottoli, I., Goller, M., and Vogt, P.K. (1999). Heparin-binding epidermal growth factor-like growth factor, a v-Jun target gene, induces oncogenic transformation. Proc. Natl. Acad. Sci. USA *96*, 5716–5721.

Green, H., and Meuth, M. (1974). An established pre-adipose cell line and its differentiation in culture. Cell *3*, 127–133.

Green, H., and Kehinde, O. (1975). An established preadipose cell line and its differentiation in culture. II. Factors affecting the adipose conversion. Cell *5*, 19–27.

Green, H., and Kehinde, O. (1976). Spontaneous heritable changes leading to increased adipose conversion in 3T3 cells. Cell *7*, 105–113.

Green, H., and Kehinde, O. (1979). Formation of normally differentiated subcutaneous fat pads by an established preadipose cell line. J. Cell. Physiol. *101*, 169–171.

Grigoriadis, A.E., Schellander, K., Wang, Z.Q., and Wagner, E.F. (1993). Osteoblasts are target cells for transformation in c-fos transgenic mice. J. Cell Biol. *122*, 685–701.

Hattori, K., Angel, P., Le Beau, M.M., and Karin, M. (1988). Structure and chromosomal localization of the functional intronless human JUN protooncogene. Proc. Natl. Acad. Sci. USA *85*, 9148–9152.

Heidenblad, M., Hallor, K.H., Staaf, J., Jonsson, G., Borg, A., Hoglund, M., Mertens, F., and Mandahl, N. (2006). Genomic profiling of bone and soft tissue tumors with supernumerary ring chromosomes using tiling resolution bacterial artificial chromosome microarrays. Oncogene *25*, 7106–7116.

Hirosumi, J., Tuncman, G., Chang, L., Gorgun, C.Z., Uysal, K.T., Maeda, K., Karin, M., and Hotamisligil, G.S. (2002). A central role for JNK in obesity and insulin resistance. Nature *420*, 333–336.

Hsu, W., Kerppola, T.K., Chen, P.L., Curran, T., and Chen-Kiang, S. (1994). Fos and Jun repress transcription activation by NF-IL6 through association at the basic zipper region. Mol. Cell. Biol. *14*, 268–276.

Hu, E., Kim, J.B., Sarraf, P., and Spiegelman, B.M. (1996). Inhibition of adipogenesis through MAP kinase-mediated phosphorylation of PPARgamma. Science *274*, 2100–2103.

Jean, S., Bideau, C., Bellon, L., Halimi, G., De Meo, M., Orsiere, T., Dumenil, G., Berge-Lefranc, J.L., and Botta, A. (2001). The expression of genes induced in melanocytes by exposure to 365-nm UVA: Study by cDNA arrays and real-time quantitative RT-PCR. Biochim. Biophys. Acta *1522*, 89–96.

Jochum, W., Passegue, E., and Wagner, E.F. (2001). AP-1 in mouse development and tumorigenesis. Oncogene *20*, 2401–2412.

Jurado, L.A., Song, S., Roesler, W.J., and Park, E.A. (2002). Conserved amino acids within CCAAT enhancer-binding proteins (C/EBP(alpha) and beta) regulate phosphoenolpyruvate carboxykinase (PEPCK) gene expression. J. Biol. Chem. *277*, 27606–27612.

Karaya, K., Mori, S., Kimoto, H., Shima, Y., Tsuji, Y., Kurooka, H., Akira, S., and Yokota, Y. (2005). Regulation of Id2 expression by CCAAT/enhancer binding protein beta. Nucleic Acids Res. *33*, 1924–1934.

Khatib, Z.A., Matsushime, H., Valentine, M., Shapiro, D.N., Sherr, C.J., and Look, A.T. (1993). Coamplification of the CDK4 gene with MDM2 and GLI in human sarcomas. Cancer Res. *53*, 5535–5541.

Kim, J.B., and Spiegelman, B.M. (1996). ADD1/SREBP1 promotes adipocyte differentiation and gene expression linked to fatty acid metabolism. Genes Dev. *10*, 1096–1107.

Lallemand, D., Ham, J., Garbay, S., Bakiri, L., Traincard, F., Jeannequin, O., Pfarr, C.M., and Yaniv, M. (1998). Stress-activated protein kinases are negatively regulated by cell density. EMBO J. *17*, 5615–5626.

Maeno, K., Masuda, A., Yanagisawa, K., Konishi, H., Osada, H., Saito, T., Ueda, R., and Takahashi, T. (2006). Altered regulation of c-jun and its involvement in anchorage-independent growth of human lung cancers. Oncogene *25*, 271–277.

Maki, Y., Bos, T.J., Davis, C., Starbuck, M., and Vogt, P.K. (1987). Avian sarcoma virus 17 carries the jun oncogene. Proc. Natl. Acad. Sci. USA *84*, 2848–2852.

Mathas, S., Hinz, M., Anagnostopoulos, I., Krappmann, D., Lietz, A., Jundt, F., Bommert, K., Mechta-Grigoriou, F., Stein, H., Dorken, B., and Scheidereit, C. (2002). Aberrantly expressed c-Jun and JunB are a hallmark of Hodgkin lymphoma cells, stimulate proliferation and synergize with NF-kappa B. EMBO J. *21*, 4104–4113.

Mercier, N., Moldes, M., El Hadri, K., and Feve, B. (2001). Semicarbazide-sensitive amine oxidase activation promotes adipose conversion of 3T3–L1 cells. Biochem. J. *358*, 335–342.

Nateri, A.S., Spencer-Dene, B., and Behrens, A. (2005). Interaction of phosphorylated c-Jun with TCF4 regulates intestinal cancer development. Nature *437*, 281–285.

Neels, J.G., Thinnes, T., and Loskutoff, D.J. (2004). Angiogenesis in an in vivo model of adipose tissue development. FASEB J. *18*, 983–985.

Oishi, Y., Manabe, I., Tobe, K., Tsushima, K., Shindo, T., Fujiu, K., Nishimura, G., Maemura, K., Yamauchi, T., Kubota, N., et al. (2005). Kruppel-like transcription factor KLF5 is a key regulator of adipocyte differentiation. Cell Metab. *1*, 27–39.

Passegue, E., and Wagner, E.F. (2000). JunB suppresses cell proliferation by transcriptional activation of p16(INK4a) expression. EMBO J. *19*, 2969–2979.

Passegue, E., Jochum, W., Schorpp-Kistner, M., Mohle-Steinlein, U., and Wagner, E.F. (2001). Chronic myeloid leukemia with increased granulocyte progenitors in mice lacking junB expression in the myeloid lineage. Cell *104*, 21–32.

Pfarr, C.M., Mechta, F., Spyrou, G., Lallemand, D., Carillo, S., and Yaniv, M. (1994). Mouse JunD negatively regulates fibroblast growth and antagonizes transformation by ras. Cell *76*, 747–760.

Poli, V., Mancini, F.P., and Cortese, R. (1990). IL-6DBP, a nuclear protein involved in interleukin-6 signal transduction, defines a new family of leucine zipper proteins related to C/EBP. Cell *63*, 643–653.

Rangatia, J., Vangala, R.K., Singh, S.M., Peer Zada, A.A., Elsasser, A., Kohlmann, A., Haferlach, T., Tenen, D.G., Hiddemann, W., and Behre, G. (2003). Elevated c-Jun expression in acute myeloid leukemias inhibits C/EBPalpha DNA binding via leucine zipper domain interaction. Oncogene *22*, 4760–4764.

Ron, D., and Habener, J.F. (1992). CHOP, a novel developmentally regulated nuclear protein that dimerizes with transcription factors C/EBP and LAP and functions as a dominant-negative inhibitor of gene transcription. Genes Dev. *6*, 439–453.

Sabatakos, G., Sims, N.A., Chen, J., Aoki, K., Kelz, M.B., Amling, M., Bouali, Y., Mukhopadhyay, K., Ford, K., Nestler, E.J., and Baron, R. (2000). Overexpression of DeltaFosB transcription factor(s) increases bone formation and inhibits adipogenesis. Nat. Med. *6*, 985–990.

Schleiermacher, G., Raynal, V., Janoueix-Lerosey, I., Combaret, V., Aurias, A., and Delattre, O. (2004). Variety and complexity of chromosome 17 translocations in neuroblastoma. Genes Chromosomes Cancer *39*, 143–150.

Schreiber, M., Kolbus, A., Piu, F., Szabowski, A., Mohle-Steinlein, U., Tian, J., Karin, M., Angel, P., and Wagner, E.F. (1999). Control of cell cycle progression by c-Jun is p53 dependent. Genes Dev. *13*, 607–619.

Schuh, A.C., Keating, S.J., Monteclaro, F.S., Vogt, P.K., and Breitman, M.L. (1990). Obligatory wounding requirement for tumorigenesis in v-jun transgenic mice. Nature *346*, 756–760.

Sebastian, T., Malik, R., Thomas, S., Sage, J., and Johnson, P.F. (2005). C/EBPbeta cooperates with RB:E2F to implement Ras(V12)-induced cellular senescence. EMBO J. *24*, 3301–3312.

Shao, D., and Lazar, M.A. (1997). Peroxisome proliferator activated receptor gamma, CCAAT/enhancer-binding protein alpha, and cell cycle status regulate the commitment to adipocyte differentiation. J. Biol. Chem. *272*, 21473–21478.

Shaulian, E., and Karin, M. (2002). AP-1 as a regulator of cell life and death. Nat. Cell Biol. *4*, E131–E136.

Shaulian, E., Schreiber, M., Piu, F., Beeche, M., Wagner, E.F., and Karin, M. (2000). The mammalian UV response: c-Jun induction is required for exit from p53-imposed growth arrest. Cell *103*, 897–907.

Student, A.K., Hsu, R.Y., and Lane, M.D. (1980). Induction of fatty acid synthetase synthesis in differentiating 3T3–L1 preadipocytes. J. Biol. Chem. *255*, 4745–4750.

Szabowski, A., Maas-Szabowski, N., Andrecht, S., Kolbus, A., Schorpp-Kistner, M., Fusenig, N.E., and Angel, P. (2000). c-Jun and JunB antagonistically control cytokine-regulated mesenchymal-epidermal interaction in skin. Cell *103*, 745–755.

Tang, Q.Q., Zhang, J.W., and Daniel Lane, M. (2004). Sequential gene promoter interactions by C/EBPbeta, C/EBPalpha, and PPARgamma during adipogenesis. Biochem. Biophys. Res. Commun. *318*, 213–218.

Toft, D.J., Rosenberg, S.B., Bergers, G., Volpert, O., and Linzer, D.I. (2001). Reactivation of proliferin gene expression is associated with increased angiogenesis in a cell culture model of fibrosarcoma tumor progression. Proc. Natl. Acad. Sci. USA *98*, 13055–13059.

Tominaga, S., Yamaguchi, T., Takahashi, S., Hirose, F., and Osumi, T. (2005). Negative regulation of adipogenesis from human mesenchymal stem cells by Jun N-terminal kinase. Biochem. Biophys. Res. Commun. *326*, 499–504.

Umayahara, Y., Kajimoto, Y., Fujitani, Y., Gorogawa, S., Yasuda, T., Kuroda, A., Ohtoshi, K., Yoshida, S., Kawamori, D., Yamasaki, Y., and Hori, M. (2002). Protein kinase C-dependent, CCAAT/enhancer-binding protein beta-mediated expression of insulin-like growth factor I gene. J. Biol. Chem. *277*, 15261–15270.

Vogt, P.K. (2001). Jun, the oncoprotein. Oncogene *20*, 2365–2377.

Weiss, C., and Bohmann, D. (2004). Deregulated repression of c-Jun provides a potential link to its role in tumorigenesis. Cell Cycle *3*, 111–113.

Wisdom, R., Johnson, R.S., and Moore, C. (1999). c-Jun regulates cell cycle progression and apoptosis by distinct mechanisms. EMBO J. *18*, 188–197.

Wu, K.K. (2003). Aspirin and other cyclooxygenase inhibitors: new therapeutic insights. Semin. Vasc. Med. *3*, 107–112.

Yeh, W.C., Cao, Z., Classon, M., and McKnight, S.L. (1995). Cascade regulation of terminal adipocyte differentiation by three members of the C/EBP family of leucine zipper proteins. Genes Dev. *9*, 168–181.

Zagariya, A., Mungre, S., Lovis, R., Birrer, M., Ness, S., Thimmapaya, B., and Pope, R. (1998). Tumor necrosis factor alpha gene regulation: enhancement of C/EBPbeta-induced activation by c-Jun. Mol. Cell. Biol. *18*, 2815–2824.

Zauberman, A., Lapter, S., and Zipori, D. (2001). Smad proteins suppress CCAAT/enhancer-binding protein (C/EBP) beta- and STAT3-mediated transcriptional activation of the haptoglobin promoter. J. Biol. Chem. *276*, 24719–24725.

Zenz, R., Scheuch, H., Martin, P., Frank, C., Eferl, R., Kenner, L., Sibilia, M., and Wagner, E.F. (2003). c-Jun regulates eyelid closure and skin tumor development through EGFR signaling. Dev. Cell *4*, 879–889.

Zhu, Y., Qi, C., Korenberg, J.R., Chen, X.N., Noya, D., Rao, M.S., and Reddy, J.K. (1995). Structural organization of mouse peroxisome proliferator-activated receptor gamma (mPPAR gamma) gene: Alternative promoter use and different splicing yield two mPPAR gamma isoforms. Proc. Natl. Acad. Sci. USA *92*, 7921–7925.

Zhu, S., Yoon, K., Sterneck, E., Johnson, P.F., and Smart, R.C. (2002). CCAAT/enhancer binding protein-beta is a mediator of keratinocyte survival and skin tumorigenesis involving oncogenic Ras signaling. Proc. Natl. Acad. Sci. USA *99*, 207–212.

Accession Numbers

The Affymetrix data observed on the 16 human tumors have been deposited in the EMBL-EBI database (http://www.ebi.ac.uk/) and are accessible through accession number E-MEXP-964.